HHS Public Access

Author manuscript

*Nat Neurosci*. Author manuscript; available in PMC 2011 September 27.

Published in final edited form as:

*Nat Neurosci*. 2011 January ; 14(1): 31–36. doi:10.1038/nn.2710.

# An evolving NGF–Hoxd1 signaling pathway mediates development of divergent neural circuits in vertebrates

**Ting Guo**[1], **Kenji Mandai**[1], **Brian G. Condie**[2], **S. Rasika Wickramasinghe**[1], **Mario R. Capecchi**[3], and **David D. Ginty**[1,4]

[1]Solomon H. Snyder Department of Neuroscience, Howard Hughes Medical Institute, Johns Hopkins University School of Medicine, Baltimore, Maryland 21205, USA

[2]Department of Genetics, University of Georgia, Athens, Georgia 30602, USA

[3]Department of Human Genetics, Howard Hughes Medical Institute, University of Utah School of Medicine, Salt Lake City, Utah 84112, USA

## Summary

Species are endowed with unique sensory capabilities encoded by divergent neural circuits. One potential explanation for how divergent circuits have evolved is that conserved extrinsic signals are differentially interpreted by developing neurons of different species to yield unique patterns of axonal connections. Although NGF controls survival, maturation and axonal projections of nociceptors of different vertebrates, whether the NGF signal is differentially transduced in different species to yield unique features of nociceptor circuits is unclear. We identified a species-specific signaling module induced by NGF and mediated by a rapidly evolving *Hox* transcription factor, *Hoxd1*. Mice lacking *Hoxd1* display altered nociceptor circuitry which resembles that normally found in chicks. Conversely, ectopic expression of *Hoxd1* in developing chick nociceptors promotes a pattern of axonal projections reminiscent of the mouse. We propose that conserved growth factors control divergent neuronal transcriptional events which mediate interspecies differences in neural circuits and the behaviors they control.

The assembly of neural circuits is instructed by phylogenetically conserved families of extracellular cues that control neuronal differentiation, axon and dendrite targeting, survival, and synaptogenesis[1–3]. Yet, it is unclear how novel neural circuits arise during evolution to encode unique behaviors among different animal species. In a classic example of extrinsic control of neural development, target-derived nerve growth factor (NGF) promotes survival, maturation, and target innervation of developing nociceptors, which are polymodal sensory neurons that innervate the skin and detect pain, temperature, touch, and itch[4]. A similar, central role of NGF in nociceptor development is highly conserved in different classes of vertebrates, including mammals and birds[5–7]. However, mammalian and avian nociceptor



[4]To whom correspondence should be addressed: dginty@jhmi.edu.

**Author Contributions**

T. G., K. M. and S. R. W. performed the experiments. B. G. C. and M. R. C. generated the *Hoxd1*$^{-/-}$ mice. T.G. and D. D. G. conceived of the project, analyzed the data and wrote the manuscript.

circuits display notable differences that likely represent beneficial evolutionary adaptations[8–9]. In mammals, for example, nociceptors form elaborate axonal endings associated with hair follicles and within the epidermis[10–11]. Such epidermal and hair-follicle-associated nociceptor endings are absent in birds and reptiles[12–14] and may represent adaptive features of mammals since their skin lacks rigid mechanical barriers, such as scales and feathers present in birds and reptiles, and is thus more directly exposed to environmental stressors[15–17]. The molecular driving forces behind the evolution of neural circuits underlying mammalian nociception, as for those mediating novel sensory, motor and cognitive functions, remain poorly understood. Here, we test the idea that the conserved NGF signal triggers species-specific patterns of nociceptor gene transcription which underlie divergent organization of vertebrate nociceptor circuits.

## Results

### A screen for genes controlled by NGF signaling in mammalian nociceptors

We first searched for evolutionarily dynamic transcriptional targets of NGF signaling pathways that may function in mammals, but not in birds, to control unique aspects of nociceptor development. NGF-dependent genes in developing mouse nociceptors were identified through three separate genome-wide screens: (1) One screen compared gene expression profiles of embryonic day (e)14.5 dorsal root ganglia (DRG) of wild-type (WT) and $Ngf^{-/-}$ mice to identify genes whose transcripts are enriched in nociceptors[18]; (2) A second screen compared e14.5 DRGs of $Bax^{-/-}$ and $Ngf^{-/-}$; $Bax^{-/-}$ mice to identify NGF-regulated genes expressed in nociceptors *in vivo* ($Bax^{-/-}$ prevents nociceptor cell death accompanying genetic deletion of *Ngf* [19].); (3) The third screen compared mouse DRG explants grown in the presence or absence of NGF for identification of NGF-dependent genes expressed in nociceptors *in vitro*. These three screens identified a large cohort of NGF-dependent genes in mouse nociceptors, including the well-characterized nociceptor genes *Ret*, *CGRP*, and *TrkA* (table S1–S3). Moreover, a cross-comparison of the three screens revealed a small number of genes that are tightly regulated by NGF both *in vivo* and *in vitro* and are potentially important for development of mouse nociceptor circuitry (Fig. 1a, b). We next used parallel cultures of mouse and chick DRGs and quantitative PCR (qPCR) analyses to determine the extent to which the avian orthologs of these identified mammalian genes are also expressed in an NGF-responsive manner in chicken nociceptors (Supplemental Fig. 1). Several observations led us to focus on one gene, which encodes the homeobox transcription factor *Hoxd1*: (1) All three genome-wide screens identified *Hoxd1* as one of the most NGF-responsive genes in mice (Fig. 1b and Table S1–S3); (2) In our cross-species comparison, *Hoxd1* was robustly induced by NGF in mouse but not chick nociceptors, in stark contrast to the majority of other NGF-controlled genes, which behaved similarly in mouse and chick nociceptors (Fig. 1c, e and Supplemental Fig. 1); (3) While most *Hox* genes encode highly conserved transcription factors critical for animal development[20], sequence comparisons suggest a high degree of divergence of *Hoxd1* between different vertebrate species (Supplemental Fig. 1 and ref. 21). Furthermore, the well-characterized expression of *Hoxd1* in the anterior neuroectoderm of lower vertebrates is absent in modern mammals[22–23], raising the possibility of a newly evolved and yet unknown function of *Hoxd1* in the mammalian lineage.

## Developmental expression of *Hoxd1* in different vertebrate species

To begin to characterize potential roles of *Hoxd1* in development and evolution of vertebrate nociceptor circuits, we first examined its pattern of expression in mouse and chick embryos. *Hoxd1* expression was readily detected in ~80% of developing nociceptors of WT mouse embryos (Fig. 1g, h) where its time of onset and peak expression are coincident with that of NGF signaling (Supplemental Fig. 2). Moreover, expression of *Hoxd1* was eliminated in genetically modified mice lacking either nociceptive neurons ($Ngf^{-/-}$) or NGF/TrkA signaling ($Ngf^{-/-}$; $Bax^{-/-}$), indicating the presence of an NGF–Hoxd1 signaling module in developing mouse nociceptors (Fig. 1d, f). Furthermore, in WT mouse embryos, nociceptors in DRGs located throughout the rostrocaudal axis express *Hoxd1* at comparable levels, a pattern that is atypical for a *Hox* gene and yet consistent with the aforementioned NGF-dependent expression of *Hoxd1* (Supplemental Fig. 2). In contrast and reflecting a lack of transcriptional activation of avian *Hoxd1* in response to NGF (Fig. 1e), *Hoxd1* mRNA was undetectable in developing chick nociceptors both before and after the onset of NGF signaling in chick embryos (Fig. 1g, h). To determine whether the NGF–Hoxd1 signaling module is present in other non-mammalian vertebrates, we examined *Hoxd1* expression in developing DRGs of the reptile green anole lizard (*Anolis carolinesis*) and the amphibian clawed frog (*Xenopus tropicalis*). Few, if any, developing nociceptors of these animals express *Hoxd1*, resembling the lack of expression in chicks (Supplemental Fig. 3). Moreover, an alignment of vertebrate genomes revealed clusters of densely packed sequence motifs surrounding the *Hoxd1* transcription unit that are highly conserved in different mammals but absent in non-mammalian genomes (Supplemental Fig. 3). Thus, while peripheral target-derived NGF supports nociceptor survival and axon extension in rodents, birds and perhaps other vertebrate species[4–7], it promotes robust expression of *Hoxd1* in mouse but not chicken nociceptors.

## Nociceptive circuitry in the skin of *Hoxd1*$^{-/-}$ mice resembles that of non-mammalian vertebrates

To determine whether *Hoxd1* mediates development of divergent nociceptor circuits *in vivo*, we next generated mice harboring a targeted deletion of *Hoxd1* (Supplemental Fig. 4). $Hoxd1^{-/-}$mice are viable, fertile and, unlike mice harboring mutations in other anterior group *Hox* genes, exhibit normal hindbrain patterning (data not shown). Intriguingly, however, the pattern of nociceptor innervation of the skin of $Hoxd1^{-/-}$ mice is abnormal and reminiscent of that which is normally observed in non-mammalian vertebrates, including birds. Our initial focus was on sensory innervation of hair follicles because hair is a distinguishing feature of mammals that represents a cold adaptation feature necessary for the prevention of heat loss[16]. Moreover, in mammalian skin, hair follicles serve as organizing centers for axons of DRG somatosensory neurons, including nociceptors[10]. In WT mice, nociceptor endings, which are strongly labeled by anti-Peripherin staining, encircle most if not all down hair follicles (Fig. 2a, b). Birds, on the other hand, have evolved feathers, and feather follicles do not possess such circular sensory endings (Fig. 2a and ref. 12). Interestingly, *Hoxd1* mutant mice exhibit a marked deficit of the Peripherin$^{+}$ axonal endings associated with hair follicles (Fig. 2b, e). A key role of *Hoxd1* in nociceptor hair afferent development is further supported by the observation that it is required for specification of

Mrgprb4$^{+}$ neurons, which constitute a unique population of mammalian nociceptors that exclusively innervate hair follicles[24]. In mice, Mrgprb4$^{+}$ neurons represent ~15% of non-peptidergic nociceptors, and their peripheral axons branch exclusively in hairy skin and encircle the neck of hair follicles[24]. In *Hoxd1*$^{-/-}$ mice, there are ~3 times more DRG sensory neurons expressing *Mrgprb4* (Fig. 2d, g). Moreover, all Mrgprb4$^{+}$ neurons in *Hoxd1*$^{-/-}$ mice abnormally express markers of peptidergic nociceptors, *CGRP* and *TrkA*, indicating impaired specification of these hair follicle-associated nociceptors (Fig. 2d, f). This nociceptor specification deficit appears to be restricted to hairy skin nociceptors as expression of molecular markers for the major subclasses of nociceptors is largely normal in *Hoxd1*$^{-/-}$ mice (Supplemental Fig. 5). Lastly, in mammals, the epidermis of non-hairy (glabrous) skin is innervated by a dense array of nociceptor endings that convey noxious chemical, mechanical, and temperature stimuli[10–11]. Such epidermal free nerve endings are absent in birds and reptiles despite the presence of dermal fibers[13–14,25], as the epidermis of these species is directly protected by mechanical barriers (scales and feathers) composed of a unique tough keratin protein that is not produced by mammals[15–17]. Strikingly, in *Hoxd1*$^{-/-}$ mice, while neuronal number and dermal fibers are present in normal abundance, there is a reduction of epidermal endings of peptidergic nociceptors (Fig. 2c, h), reminiscent of that which is normally found in the skin of non-mammalian vertebrates. Thus, NGF-dependent expression of *Hoxd1* in mammalian nociceptors controls mammal-specific features of nociceptor development, including specification and target innervation of subsets of hair-follicle-associated nociceptors and penetration of the epidermis by peptidergic nociceptors.

### *Hoxd1* instructs nociceptor central axonal projections within the mammalian spinal cord

Mirroring species-specific differences in innervation of the skin, the patterns of nociceptive axonal projections within the spinal cords of mammals and birds are also distinct[8–9]. In mice, the majority of central axonal branches of nociceptors penetrate the dorsal spinal cord in the dorsal region, project ventrally, and terminate in lamina I and II of the dorsal horn (Supplemental Fig. 6). In contrast, avian (chick) nociceptors penetrate the spinal cord from a more lateral position and, in addition to those nociceptors that terminate in lamina I and II of the dorsal horn, many nociceptor axons extend horizontally into deep layers of the spinal cord[9] to innervate integrative regions that receive a convergence of sensory inputs of multiple modalities[26–27] (Supplemental Fig. 7). Remarkably, in *Hoxd1*$^{-/-}$ mice, we detected a large number of aberrant nociceptor axonal projections within the spinal cord that bear intriguing similarity to the horizontally-extending deep projections normally observed in birds (Fig. 3a, b). The aberrant nociceptor axons enter the spinal cord of *Hoxd1*$^{-/-}$ mice from a lateral position, project horizontally across the spinal cord, and enter deep regions near the central canal (Fig. 3a). These misrouted fibers are detected at all axial levels (Fig. 3c, d) and terminate in and around lamina X, an area purported to integrate somatic and visceral sensory information of multiple modalities[26–27]. Although such deep fibers were rarely observed in WT mice, the few that were seen were largely restricted to lumbrosacral levels (L4-S1; Supplemental Fig. 6) and are likely to be visceral organ afferents[28–29]. In further support of a role of NGF-dependent *Hoxd1* expression in directing nociceptor connections within the mouse spinal cord, mutant mice deficient for NGF signaling (*Ngf*$^{-/-}$; *Bax*$^{-/-}$) similarly exhibit excessive nociceptor axons within deep spinal cord layers (Fig. 4).

Moreover, consistent with this, lizards, which do not express *Hoxd1* in nociceptors (Supplemental Fig. 3), exhibit deep-projecting nociceptor fibers similar to those in chicks and *Hoxd1*$^{-/-}$ mice[30]. These observations suggest that *Hoxd1* mediates NGF-dependent suppression of nociceptor projections into deep layers of the spinal cord.

## Ectopic *Hoxd1* expression in chick nociceptors induces mammal-like traits

If NGF-dependent expression of *Hoxd1* is indeed a determinant of the mammal-specific pattern of nociceptor circuits, then ectopic expression of *Hoxd1* in non-mammalian nociceptors may alter their axonal projections to adopt mammal-like features. Therefore, we asked whether ectopic *Hoxd1* expression in nociceptors of the chick is sufficient to alter their pattern of axonal projections within the spinal cord. Using a neural crest-specific driver[31], *Hoxd1* was ectopically expressed in chick DRGs on one side of the animal, leaving the other side as a control (Fig. 5a, b), an approach that enables a direct comparison of sensory afferent projections between the electroporated and unelectroporated sides of the spinal cord[32]. Remarkably, ectopic expression of chick *Hoxd1* affected the pattern of chick nociceptor central projections (Fig. 5c–e). In control embryos, at stage 35, TrkA$^{+}$ nociceptor central axons have penetrated the superficial dorsal horn at a lateral position and have projected into deep layers of the dorsal horn. Many of these axons that initially project horizontally then turn in a ventral direction and form prominent bundles of horizontally-projecting axons (Fig. 5c and Supplemental Fig. 8). Following ectopic expression of *Hoxd1* in chick DRGs, however, the prominent deep nociceptor projections, which under normal conditions extend horizontally toward the central canal, are suppressed (Fig. 5c). Importantly, electroporation of a *Hoxd1* construct lacking the DNA-binding homeobox motif (*Hoxd1*Δ*h*) had no effect on nociceptor projections (Fig. 5d). Moreover, the central projections of proprioceptive neurons appear normal following ectopic *Hoxd1* expression (Supplemental Fig. 8). Thus, ectopic expression of *Hoxd1* alters the central projection programs of chick nociceptors, forcing them to adopt murine nociceptor features (Fig. 5e).

## *Hoxd1*$^{-/-}$ mice have deficits in pain sensitivity

To assess the behavioral consequences that may result from aberrant nociceptor circuits in *Hoxd1*$^{-/-}$ mice, we examined the *Hoxd1*$^{-/-}$ mutants for potential defects in somatosensation. Adaptation to cold climates is a central theme of mammalian evolution[33], and many evolutionarily novel features of mammals are related to cold adaptation[34]. Indeed, the ancestors of modern mammals survived and flourished during extended geological periods of cold temperatures when many terrestrial heterothermic species became extinct[35–36]. Remarkably, using measurements of avoidance of extreme hot and cold temperatures, we found that *Hoxd1*$^{-/-}$ mice exhibit markedly longer latencies of avoidance to an extremely cold (0°C) surface (Fig. 6a), representing a defective self-protection behavior essential for the survival of animals that explore cold environments[37]. *Hoxd1*$^{-/-}$ mice are otherwise comparable to littermate controls in their responses to hot temperature and light mechanical stimulation (Fig. 6b–e), although they do show abnormally prolonged carrageenan-induced thermal allodynia (Fig. 6f), suggesting a role of Hoxd1 in inflammatory pain. The causes of the behavioral deficits of *Hoxd1*$^{-/-}$ mice are uncertain; Such deficits may arise from defects in axonal wiring in the skin, the spinal cord, or in defective specification of nociceptive

neurons in the mutant mice. These results indicate that *Hoxd1* is essential for the development of behavioral responses to cold temperatures in mice.

## Discussion

Here, we report that *Hoxd1* is a rapidly evolving NGF/TrkA signaling pathway component whose differential expression in developing nociceptors across vertebrate species contributes to species-specific features of nociceptor circuits. We identified *Hoxd1* from a genome-wide screen for genes expressed in response to NGF signaling in mice but not chickens. Moreover, genetic manipulations in mammals and birds showed that *Hoxd1* instructs development of mammal-specific features of nociceptive neural circuitry. Finally, behavioral sensitivity to extreme cold is markedly compromised in *Hoxd1* mutant mice, supporting functional significance of acquisition of Hoxd1 by mammalian nociceptors.

The *Hox* genes have undergone extraordinary evolutionary selection to delineate variations of body and limb plans in divergent lineages across the animal kingdom[20]. The present study presents a particularly fascinating feature of *Hox* gene divergence such that in the mammalian lineage the conserved axial patterning functions of *Hoxd1* are lost and replaced by a role in mediating development of nociceptor circuits. Redundancy between *Hoxa1*, *Hoxb1* and *Hoxd1* may have allowed for relaxation of *Hoxd1* from conserved roles and to evolve novel functions in mammals. Loss of *Hoxd1* in mice results in compromised responses to extremely cold temperatures, an environmental stress that has challenged terrestrial animals throughout recent geological history[35–36]. Repeated, dramatic, and long-term global cooling in the Cenozoic Era may thus represent selective pressure for mammalian evolution of *Hoxd1*. More generally, our analysis indicates that altered expression of a single, evolutionarily dynamic transcription factor during the course of vertebrate evolution can instruct unique features of sensory circuits and the behaviors they subserve.

We show that mammalian features in nociceptor circuits are subject to coordinated developmental control by mammal-specific expression of *Hoxd1*. Remarkably, *Hoxd1* stands out as one gene that is robustly induced by NGF/TrkA signaling in rodents but not in birds amid a largely conserved genomic transcriptional response to NGF. We propose a model in which divergent expression of one or a small number of genes in embryos of different species, induced by conserved growth factor signaling pathways, results in macroscopic interspecies differences in adult neural circuits. Thus, identification and characterization of differentially expressed effectors of conserved growth factor signaling pathways will likely reveal key determinants of anatomical features, behaviors, and diseases unique to divergent vertebrate organ systems.

## Methods

### Generation of Mice and Mouse Genetics

*Hoxd1*$^{-/-}$ mice were generated by a targeting strategy similar to those described for several other *Hox* genes[6–7]. A *pol*II-*Neo-HPRT-pA* cassette was inserted into the second exon of the *Hoxd1* locus disrupting most of the homeobox domain including the DNA recognition helix

and sequences downstream (Supplemental Fig. 4a). Positive 129/Sv ES cell clones confirmed by Southern hybridization (Supplemental Fig. 4b) were used to generate *Hoxd1*$^{+/-}$ founders that were confirmed by Southern blot, *in situ* hybridization, and PCR of genomic DNA extracted from the tails (Supplemental Fig. 4b–d). *Hoxd1*$^{-/-}$ mice were genotyped using a multiplex PCR reaction with the following primers: 5′-TCAGAAAATGCCCCAGGAGC (forward), 5′-TAGCCGTTATTAGTGGAGAGG (mutant reverse) and 5′-TGGAACCAGATTTTGACCTGG (WT reverse). The *Ngf*$^{+/-}$ and *Bax*$^{+/-}$ alleles have been described previously[8–9]. For all of our analyses, the morning after coitus was designated as embryonic day (e)0.5 and the day of birth as postnatal day (P)0.

All experimental procedures involving animals have been approved by the IACUC of Johns Hopkins University.

## Microarray Analyses

DRGs were dissected out from e14.5 (1) *Ngf*$^{-/-}$; *Bax*$^{-/-}$, (2) *Bax*$^{-/-}$ and (3) *Ngf*$^{-/-}$ mouse embryos and (4) their control WT littermates from multiple litters and were stored in RNAlater (Ambion) at −20°C until use. DRG explants that were cultured either with NGF or with NT3 were also collected (see below). Two independent replicates, each consisting of DRGs pooled from multiple embryos of like genotypes from different litters, were separately prepared. At least 5 μg of total RNA was isolated from each group of pooled DRGs using an RNeasy Micro Kit (Qiagen). RNA was then hybridized to Affymetrix GeneChip Mouse Genome 430 2.0 arrays by the JHMI Microarray Core Facility. Statistical analyses were performed essentially as previously described[18,39].

A loose cutoff at a posterior probability > 0.5 (ref. [39]) and an estimated mRNA fold change > 1.5 was used to generate the Venn diagram (Fig. 1a). The 14 unique genes identified in all three independent microarray screens are: *Aldoc*, *Crtac1*, *Dgkh*, *Hoxd1*, *Idi1*, *Klf7*, *Nrxn1*, *Pou4f2*, *Ppp1r*, *Prkca*, *Ret*, *Rgs4*, *Rgs7* and *Tle4*. These 14 genes and other select candidate genes were tested by qPCR for NGF-responsiveness in mouse and chick DRG cultures unless the sequences for chicken orthologs were not available.

## DRG Neuron Explant Culture

For microarray analysis, DRGs were dissected out from 4 litters of e13.5 mouse embryos, placed on plates coated with poly-D-lysine and laminin, and maintained for 48 hrs with 50 ng/ml of either NGF or NT3. DRGs were then collected, and total RNA was extracted for two independent sets of cultures and processed for microarray analysis.

For expression comparisons, DRG explant culture conditions and protocols were previously described[40]. Briefly, DRGs were dissected from e13.5 mouse embryos and e7.25 chick embryos, placed on coverslips coated with collagen, and cultured with media containing 25 ng/ml NGF for 36 hours. DRG explants were then washed, deprived of NGF by culturing with BAF and anti-NGF antibody for 24 hrs, re-washed, and further cultured with BAF and either with or without NGF for an additional 24 hrs.

## Chick, Frog and Reptile Embryos and cDNAs

Chicken (*Gallus gallus*), clawed frog (*Xenopus tropicalis*), and green anole lizard (*Anolis carolinesis*) embryos were collected and staged[1,13–14]. Total RNA was extracted from stage 21~22 chicken and stage 52 frog embryos and first-strand cDNA synthesis was performed from the RNA using oligo(dT) primers and SuperScript III system (Invitrogen). A cDNA library of stage 7 *Anolis carolinesis* embryos was a generous gift from Dr. Thomas Sanger (Harvard University). Lizard and frog *TrkA* genes are identified based on homology searches using the highly conserved kinase domain, and lizard *Hoxd1* was identified by homology and the genomic structure of the *HoxD* cluster and is in agreement with previous reports[41]. PCR products were blunt-end cloned into a *pSC-B* vector (Stratagene) and used as templates for synthesis of *in situ* hybridization probes. The following primers were used to amplify fragments of the *TrkA* and *Hoxd1* genes from the cDNA.

Frog *TrkA*: 5′-GATAATCCCTTCAGCTTTAACC and 5′-ATCTTGACCACCAGATTATTGC

Frog *Hoxd1*: 5′-GAAAGATTGAGGGATCATCAGG and 5′-TCGAGTTCAGTCAGTTGTTTGG

Lizard *TrkA*: 5′-CACCGAAGAGAAGATGCTGGT and 5′-TAAATACACCGGGGGAGCTTT

Lizard *Hoxd1*: 5′-AAGCAGAAGAAAAGGGAGAGAGA and 5′-TGTAAGTGAAGTTGGGGAGAGAA

## Immunohistochemistry and *In Situ* Hybridization

Protocols for immunohistochemistry and *in situ* hybridization were essentially as described[38]. For immunohistochemistry, mouse tissues were either preserved directly in OCT (Tissue Tek), fixed or transcardially perfused with either 4% ice-cold paraformylaldehyde (PFA) or Zamboni's fixative then cryoprotected in 30% sucrose/phosphate-buffered saline (PBS). Immunofluorescent stainings were performed with cryosections either on glass slides or as floating sections. Primary antibodies used include: rabbit anti-mouse TrkA (Millipore, 1:1000), rabbit anti-chicken TrkA and TrkC (gifts from Dr. Frances Lefcort, Montana State University, 1:1000), rabbit (Millipore, 1:1000) or mouse anti-peripherin (Millipore, 1:500), rabbit anti-CGRP (Millipore, 1:1000), rabbit anti-PGP9.5 (Millipore, 1:1000), rabbit anti-Parvalbumin (Swant, 1:2000), rabbit anti-GFP (1:2000, Invitrogen), chicken anti-LacZ (Promega, 1:500), rabbit anti-Ret (Immuno-Biological Laboratories, 1:1000), mouse anti-chick Neurofilament 160kD (Zymed, 1:500) and rabbit anti-Neurofilament 200 (Millipore, 1:1000). Secondary antibody incubations were performed with Alexa Fluor-conjugated secondary antibodies (Molecular Probes, 1:500).

Probes used for *in situ* hybridization were: mouse *Hoxd1* (nucleotides 946–1386 of NM_010467.2), mouse *CRD-Nrg1* (nucleotides 1–598 of NM_178591.2), rat *Nrp1* (nucleotides 2515–3799 of NM_145098), chick *Hoxd1* (BU269116, (clone ChEST816c12, GeneServices) digested by PstI and transcribed with T3) and frog *Hoxd1* (nucleotides 7–701 of NM_001016678.2). Sequences of *in situ* probes for lizard *Hoxd1* and lizard *TrkA* are described above in the "Chick, Frog and Reptile Embryos and cDNAs" section.

### Imaging, Quantification and Statistical Analyses

Confocal fluorescent images were taken on a Zeiss Axioskop 2 microscope with an LSM 510 confocal scanning module. Whole-mount fluorescent images were taken from a Zeiss SteREO Lumar.V12 fluorescent dissecting microscope. To quantify hairy skin innervation, an approximately 4 mm X 4 mm piece of the back thigh hairy skin was dissected from young adult animals (P20 – P30), and serial cryosection was performed at a thickness of 25 μm. Every third or fifth section was collected, and the total number of circular hair follicle endings was counted in each of the collected sections. The number was then normalized to the area of the skin measured in ImageJ. The same skin region was taken from each animal. Quantification of epidermal free nerve endings was performed as described[38]. Fluorescent intensities were measured using ImageJ (NIH), and a rectangular measuring window with the same size was applied to all images that were compared. The statistical analyses of significance, including *p* value cutoffs, are specified in Figure Legends.

### Quantitative RT-PCR

First-strand cDNA was synthesized from 1 μg of total tissue RNA using oligo(dT) primers and SuperScript III First Strand Synthesis System (Invitrogen). Real-time PCR (qPCR) was performed using an Applied Biosystems 7300 Real-Time PCR System using Quantitect SYBR Green PCR Kit (Qiagen). Expression levels for each gene from each sample were normalized to control PCR products of *Gapdh* or *Actb* for non-neuronal tissues, or *Pgp9.5* (alias *Uchl1*) specifically for neurons[18]. Primers for qPCR were:

Mouse *Hoxd1*: 5′-CCCCAAGAAAAGCAAACTGTCC and 5′-AAACAGTTGGCTATCTCGATGC;

Chicken *Hoxd1*: 5′-AGAGGAGGAGCAGAAACCCCAG and 5′-TTTGCACAGGAAGGGAGGAAGAC;

Mouse *Ret*: 5′-AGAAAAGCAAGGGCCGGATTC and 5′-GTCGTTCAGGAGGAATTCCAGG;

Chicken *Ret*: 5′-AAAGTGATGTGTGGTCGTTTGG and 5′-CACTGCAGTTTTCTGGTCTCTCC;

Mouse *CGRP*: 5′-AGGGCTCTAGTGTCACTGCTCAG and 5′-CACATTGGTGGGAACAAAGTTG;

Chicken *CGRP*: 5′-CAGTCAGACCTGGCTTGGAGTC and 5′-TGTTCCCCTCAGAGGCTTGCTC;

Mouse *Klf7*: 5′ - GAGCTCGGGGGAGGGTTTCTCC and 5′ - GCCGGTGTCGTGGACAAGTTGT

Chicken *Klf7*: 5′ – TGGCAGCAGACATGCCTCGAGT and 5′ - GGGGTCCAGCCGTCGGATACTG

Mouse *Ldb2*: 5′ - GCACGTCCAATAGCAGTGCCGG and 5′ - TCCTACCACCATCACATCAGGTACCT

Chicken *Ldb2*: 5′ - TCCAGCGCACCACATGACCCTT and 5′ - GTTGTCACTGTCCTCGCTCCGC

Mouse *Diras2*: 5′ - GGACCGTGAGCCTCCAGATCGA and 5′ - TCCTGCACGAAGGCCTCTCACA

Chicken *Diras2*: 5′ - GTGGTTGTGTTTGGGGCTGGAGG and 5′ - TGCCGGTAGGTGTCTTCAATGGTG

Mouse *Ncam2*: 5′ - GCAAAGTAGAGCTTAGTGTGGGTGAG and 5′ - GTCGTGACCTGACACCCTCCTT

Chicken *Ncam2*: 5′ - AGCAAAGTCGAACTCAGTGTGGGT and 5′ - ACGTGACCGAACACCTTCTTTTTGA

Mouse *Nrxn1*: 5′ - AGAAGGAAGCCGTGTTGGTGCG and 5′ - CGATGGCGATGTCATCTGTCCCA

Chicken *Nrxn1*: 5′ - TCGTACAACTGAGCCAAATGGTTTGA and 5′ – ACAGCAGGTAGAGGTGGCCATCA

Mouse *Runx1*: 5′ - CTCCAGCCTCCAGCTACTGCCC and 5′ - CCTGAGCCTGACAGTGCCCCTT

Chicken *Runx1*: 5′ - TGGAAGAGGGAAAAGCTTCACAC and 5′ – CTTGCCTCGTGTTTCTGGGTTC

Mouse *Rgs7*: 5′ - ACGGAGCCATCGCCCATACCTT and 5′ - ACAGCGTCCCTTGGCAAGTGTG

Chicken *Rgs7*: 5′ - GCTGGTGTACAGAAAGATGGAAGACG and 5′ - TGTCTGAACCAGAAAAGACACTGGGG

Mouse *PlxnC1*: 5′ – TGCCTGGCCCATCTAGACTGCA and 5′ - ACAAGATTGGGAGGGCGTCTGT

Chicken *PlxnC1*: 5′ – TGCAGTGTCCAAAATGCTTCCAAGG and 5′ - TGCCCAACGTAGAAATCCACAAAGGC

Mouse *Ppp1r*: 5′ - AGCATGCTTCTGTGGACTCCCCA and 5′ - AGGTTTAGCACCCACCTCCATGGT

Chicken *Ppp1r*: 5′ – GAGTGCCTGTGCTACTCGCACC and 5′ - CCCCAAGTGAGCAGATCACCAGC

Mouse *Prkca*: 5′ - CCCACAGCGGGATTTTCCCGTG and 5′ - CCGTCATCCCCACAGTTGAGCG

Chicken *Prkca*: 5′ – GGGACAGTTGGTGAGCGAACCG and 5′ - AAATCCCAGGCGCCAAAGGACG

Mouse *Crtac1*: 5′ – TGATGGGGGTTCCGGCTACCTG and 5′ - GGCCACACTTCGGCTCACCATC

Chicken *Crtac1*: 5′ - CGAGAACGGACGCTGCGTAGAC and 5′ - AGCGGTACCCGCCATAGGTGTT

Mouse *Etv4*: 5′ – ATGCAGAAGGTGGCTGGCGAAC and 5′ - TGTCCTCCTCACTGACTGGCCG

Chicken *Etv4*: 5′ - GCTGTGCCATGTGGCTGCAAAC and 5′ - CAGGCAAGGAGGTGGCAATGCA

Mouse *Rgs4*: 5′ - GCCAATGTACCGGGCTGCAAAA and 5′ - GATGGGGGAGCTCTGGGGACAT

Chicken *Rgs4*: 5′ – CTCGTTCCTGCTCCTGGGCTCT and 5′ - TGCCGTGTCAGAACCCCTGTGA

Mouse *Tle4*: 5′ - AGGACTGCTTGCCTACCGCTGT and 5′ - TAAAGCAAGCCACCATCCCGGG

Chicken *Tle4*: 5′ - AGTACATTGTCACTGGCTCTGGGG and 5′ - AGTGCTAGGAGAAGGAGTTCTGCCT

Mouse *Dgkh*: 5′ - AGCCATCAACGTCAAGGCGCTC and 5′ - TGTAAGGCACTGGACACCCGCT

Chicken *Dgkh*: 5′ – ACTGCAGCACCACCGGATAGCT and 5′ - CTCCTGGGGGCTGGATCCATGC

Mouse *Pou4f2*: 5′ - CGGCACACGTGCTCTCTCACTC and 5′ - TGGAGACTGCACCTAAGGCTGGG

Chicken *Pou4f2*: 5′ - ACTCTTGGAGCACCTGACGCCG and 5′ - ATGGGGTTCATGCCGGCCATG

Chicken *Gapdh*: 5′-GAAGGCTGGGGCTCATCTGAAG and 5′-CACGATGCATTGCTGACAATTTTC;

Mouse *Gapdh*: 5′-ACTGTGGTCATGAGCCCTTC and 5′-CATGTTTGTGATGGGTGTGAAC;

Mouse *Pgp9.5*: 5′-ACGGCCCAGCATGAAAACT and 5′-GACGGATCCATCCTCAAATTCC;

Mouse *Actb*: 5′-CCACTGCCGCATCCTCTTCC and 5′-CTCGTTGCCAATAGTGATGACCTG.

### Chick *In Ovo* Electroporation

Chick *in ovo* electroporation was performed as described[42–43]. Briefly, DNA was injected into the neural tube of Hamburger & Hamilton (HH) stage 12~13 chick embryos using a glass pipette. Electrical field was then applied with a pair of needle electrodes (Genetrodes; Harvard Apparatus) and a square pulse electroporator (BTX) at 30 V (pulse length: 50 ms; number of pulses: 5; intervals: 1 s). Successfully electroporated eggs, visually confirmed by endogenous GFP signal under a Zeiss SteREO Lumar.V12 fluorescent dissecting microscope 2 or 3 days after electroporation, were incubated until stage 34~35 for analysis.

Chicken *Hoxd1* coding sequence was amplified from a chicken cDNA library with: 5′-ATGGACTTGGGTTTTTTCCC (Forward) and 5′-TCAATACAAAGGGAGTAAAGCAGC (Reverse). Truncated chick *Hoxd1* lacking homeobox was amplified with the same forward primer and 5′-CTGCCGGGTGCTGAAACTG (Reverse).

To achieve selective expression in the DRGs, we used a strategy similar to what has been demonstrated for motor neuron-specific electroporation[18] but instead searched for enhancers that direct DRG-specificity. Briefly, two constructs were co-electroporated: the first was electroporated at a lower concentration (0.2 μg/μl) and uses an enhancer connected to a weak basal promoter (*CMV*) to drive *Cre* recombinase expression. The second construct, electroporated at a high concentration (1~2 μg/μl), uses a strong promoter (*CAGGS*) to drive a *lox*P-*STOP*-*lox*P-*GeneX*-*IRES*-*eGFPf* cassette. Over 10 enhancer fragments that direct DRG-specific expression in transgenic mice were tested, and one fragment of the *Sox10* enhancer (“D6”, described in ref. [31]) was used. Primers used to clone this fragment from mouse genomic DNA were: 5′-ATGACCGTAAGCCTTAGGAGATGG (Forward) and 5′-GCACTGGCATAGTTGGAAGAATGG (Reverse).

### Pain Behavioral Tests

Pain behavioral tests were done essentially as described[44]. Briefly, for the Hargreaves’ test (radiant heat), mice were placed in plexiglas restrainers and a light beam was directed to the footpads of hindpaws using an IITC Plantar Analgesia Meter. For tail immersion, mice were gently restrained in a specially machined 50 ml conical tube that permits ventilation, and the distal halves of their tails were immersed in a 50 °C water bath. For the hot plate test, mice were placed in an IITC Hot Plate Analgesia Meter, and the onset of brisk paw lifts and/or flicking/licking of the paw was assessed. For cold plate, a clear Plexiglas cylinder was placed on a metallic plate equilibrated to 0 °C, and mice were placed inside the cylinder. The latency to the onset of brisk and persistent paw withdrawal and/or licking of the paw was measured. For the von Frey assay, mice were placed within Plexiglas restrainers on a fine metallic grid, and their hindpaws were stimulated using a set of von Frey filaments (Bioseb) starting with the lowest force. For carrageenan-induced inflammation, 10 μl of 1 % carrageenan (Sigma 22049) dissolved in sterile saline was injected subcutaneously into right hindpaws using a Hamilton syringe, and thermal hyperalgesia was measured using a Hargreaves’ apparatus before, 6 hrs, and 24 hrs after the injection. All mice used for behavioral studies were 2~3 month old and were backcrossed to the 129/Sv mouse strain for at least 4 generations.

## Supplementary Material

Refer to Web version on PubMed Central for supplementary material.

## Acknowledgments

We thank T. Sanger for green anole embryos, cDNA, and assistance with staging, N. Marsh-Armstrong for frog embryos, F. Lefcort for antibodies, S. Sockanathan, B. Zhuang, and C. Lee for reagents and technical assistance with chick electroporation, A. Kolodkin, M. Li, X. Dong and H. Song for helpful discussions, and members of the Ginty lab for comments on the manuscript, discussions, and assistance throughout the course of the project. This

work is supported by NIH grant NS34814 (DDG). M.R.C. and D.D.G are investigators of the Howard Hughes Medical Institute.

## References

1. Dodd J, Jessell TM. Axon guidance and the patterning of neuronal projections in vertebrates. Science (New York, NY). 1988; 242:692–699.
2. Tessier-Lavigne M, Goodman CS. The molecular biology of axon guidance. Science (New York, NY). 1996; 274:1123–1133.
3. Huber AB, Kolodkin AL, Ginty DD, Cloutier JF. Signaling at the growth cone: ligand-receptor complexes and the control of axon growth and guidance. Annual Review of Neuroscience. 2003; 26:509–563.
4. Snider WD. Functions of the neurotrophins during nervous system development: what the knockouts are teaching us. Cell. 1994; 77:627–638. [PubMed: 8205613]
5. Huang EJ, Reichardt LF. Neurotrophins: roles in neuronal development and function. Annual Review of Neuroscience. 2001; 24:677–736.
6. Levi-Montalcini R. The nerve growth factor 35 years later. Science (New York, NY). 1987; 237:1154–1162.
7. Gundersen RW, Barrett JN. Neuronal chemotaxis: chick dorsal-root axons turn toward high concentrations of nerve growth factor. Science (New York, NY). 1979; 206:1079–1080.
8. Mirnics K, Koerber HR. Prenatal development of rat primary afferent fibers: II. Central projections. The Journal of comparative neurology. 1995; 355:601–614. [PubMed: 7636034]
9. Eide AL, Glover JC. Developmental dynamics of functionally specific primary sensory afferent projections in the chicken embryo. Anatomy and Embryology. 1997; 195:237–250. [PubMed: 9084822]
10. Rice, FL.; Albrecht, PJ. The Senses: A Comprehensive Reference. 6. Basbaum, AI.; Kaneko, A.; Shepherd, GM.; Westheimer, G., editors. Academic Press; 2008. p. 1-32.
11. Zylka MJ, Rice FL, Anderson DJ. Topographically distinct epidermal nociceptive circuits revealed by axonal tracers targeted to Mrgprd. Neuron. 2005; 45:17–25. [PubMed: 15629699]
12. Lucas, AM.; Stettenheim, PR. Avian anatomy - Integument. Vol. 2. United States Department of Agriculture; 1972. p. 361
13. Hemming FJ, Pays L, Soubeyran A, Larruat C, Saxod R. Development of sensory innervation in chick skin: comparison of nerve fibre and chondroitin sulphate distributions in vivo and in vitro. Cell and tissue research. 1994; 277:519–529. [PubMed: 7954688]
14. Von During, M.; Miller, ML. Biology of the Reptilia. 9. Gans, Carl, editor. Academic Press; 1979. p. 407-441.
15. Chuong CM, Chodankar R, Widelitz RB, Jiang TX. Evo-devo of feathers and scales: building complex epithelial appendages. Curr Opin Genet Dev. 2000; 10:449–456. [PubMed: 11023302]
16. Wu P, et al. Evo-Devo of amniote integuments and appendages. Int J Dev Biol. 2004; 48:249–270. [PubMed: 15272390]
17. Chang C, et al. Reptile scale paradigm: Evo-Devo, pattern formation and regeneration. Int J Dev Biol. 2009; 53:813–826. [PubMed: 19557687]
18. Mandai K, et al. LIG family receptor tyrosine kinase-associated proteins modulate growth factor signals during neural development. Neuron. 2009; 63:614–627. [PubMed: 19755105]
19. Patel TD, Jackman A, Rice FL, Kucera J, Snider WD. Development of sensory neurons in the absence of NGF/TrkA signaling in vivo. Neuron. 2000; 25:345–357. [PubMed: 10719890]
20. Pearson JC, Lemons D, McGinnis W. Modulating Hox gene functions during animal body patterning. Nature reviews Genetics. 2005; 6:893–904.
21. Tvrdik P, Capecchi MR. Reversal of Hox1 gene subfunctionalization in the mouse. Developmental cell. 2006; 11:239–250. [PubMed: 16890163]
22. Frohman MA, Martin GR. Isolation and analysis of embryonic expression of Hox-4.9, a member of the murine labial-like gene family. Mechanisms of development. 1992; 38:55–67. [PubMed: 1356009]

23. Kolm PJ, Sive HL. Regulation of the Xenopus labial homeodomain genes, HoxA1 and HoxD1: activation by retinoids and peptide growth factors. Developmental biology. 1995; 167:34–49. [PubMed: 7851655]
24. Liu Q, et al. Molecular genetic visualization of a rare subset of unmyelinated sensory neurons that may detect gentle touch. Nat Neurosci. 2007; 10:946–948. [PubMed: 17618277]
25. Saxod, R. Handbook of Sensory Physiology. In: Jacobson, M., editor. Development of Sensory Systems. Vol. IX. Springer-Verlag; 1978. p. 338
26. Wall PD, Kerr BJ, Ramer MS. Primary afferent input to and receptive field properties of cells in rat lumbar area X. The Journal of comparative neurology. 2002; 449:298–306. [PubMed: 12115681]
27. Honda CN. Visceral and somatic afferent convergence onto neurons near the central canal in the sacral spinal cord of the cat. Journal of neurophysiology. 1985; 53:1059–1078. [PubMed: 3998792]
28. Nadelhaft I, Roppolo J, Morgan C, de Groat WC. Parasympathetic preganglionic neurons and visceral primary afferents in monkey sacral spinal cord revealed following application of horseradish peroxidase to pelvic nerve. The Journal of comparative neurology. 1983; 216:36–52. [PubMed: 6306063]
29. Chung K, Lee WT, Park MJ. Spinal projections of pelvic visceral afferents of the rat: a calcitonin gene-related peptide (CGRP) immunohistochemical study. The Journal of comparative neurology. 1993; 337:63–69. [PubMed: 8276992]
30. Martinez-Garcia F, Novejarque A, Landete JM, Moncho-Bogani J, Lanuza E. Distribution of calcitonin gene-related peptide-like immunoreactivity in the brain of the lizard Podarcis hispanica. J Comp Neurol. 2002; 447:99–113.10.1002/cne.10200 [PubMed: 11977114]
31. Werner T, Hammer A, Wahlbuhl M, Bosl MR, Wegner M. Multiple conserved regulatory elements with overlapping functions determine Sox10 expression in mouse embryogenesis. Nucleic acids research. 2007; 35:6526–6538. [PubMed: 17897962]
32. Chen AI, de Nooij JC, Jessell TM. Graded activity of transcription factor Runx3 specifies the laminar termination pattern of sensory axons in the developing spinal cord. Neuron. 2006; 49:395–408. [PubMed: 16446143]
33. Kemp, TS. The origin and evolution of mammals. Oxford University Press; 2005.
34. Kardong, KV. Vertebrates: comparative anatomy, function, evolution. McGraw-Hill Higher Education; 2006.
35. Zanazzi A, Kohn MJ, MacFadden BJ, Terry DO. Large temperature drop across the Eocene-Oligocene transition in central North America. Nature. 2007; 445:639–642. [PubMed: 17287808]
36. Prothero, DR.; Berggren, WA. Eocene-Oligocene Climatic and Biotic Evolution. Princeton Univ. Press; 1992.
37. Kim SJ, Qu Z, Milbrandt J, Zhuo M. A transcription factor for cold sensation! Mol Pain. 2005; 1:11. [PubMed: 15813958]
38. Luo W, et al. A hierarchical NGF signaling cascade controls Ret-dependent and Ret-independent events during development of nonpeptidergic DRG neurons. Neuron. 2007; 54:739–754. [PubMed: 17553423]
39. Deppmann CD, et al. A model for neuronal competition during development. Science. 2008; 320:369–373. [PubMed: 18323418]
40. Lonze BE, Riccio A, Cohen S, Ginty DD. Apoptosis, axonal growth defects, and degeneration of peripheral neurons in mice lacking CREB. Neuron. 2002; 34:371–385. [PubMed: 11988169]
41. Di-Poi N, Montoya-Burgos JI, Duboule D. Atypical relaxation of structural constraints in Hox gene clusters of the green anole lizard. Genome research. 2009; 19:602–610. [PubMed: 19228589]
42. Nakamura H, Funahashi J. Introduction of DNA into chick embryos by in ovo electroporation. Methods (San Diego, Calif). 2001; 24:43–48.
43. Zhuang B, Su YS, Sockanathan S. FARP1 promotes the dendritic growth of spinal motor neuron subtypes through transmembrane Semaphorin6A and PlexinA4 signaling. Neuron. 2009; 61:359–372. [PubMed: 19217374]
44. Liu Q, et al. Sensory neuron-specific GPCR Mrgprs are itch receptors mediating chloroquine-induced pruritus. Cell. 2009; 139:1353–1365. [PubMed: 20004959]

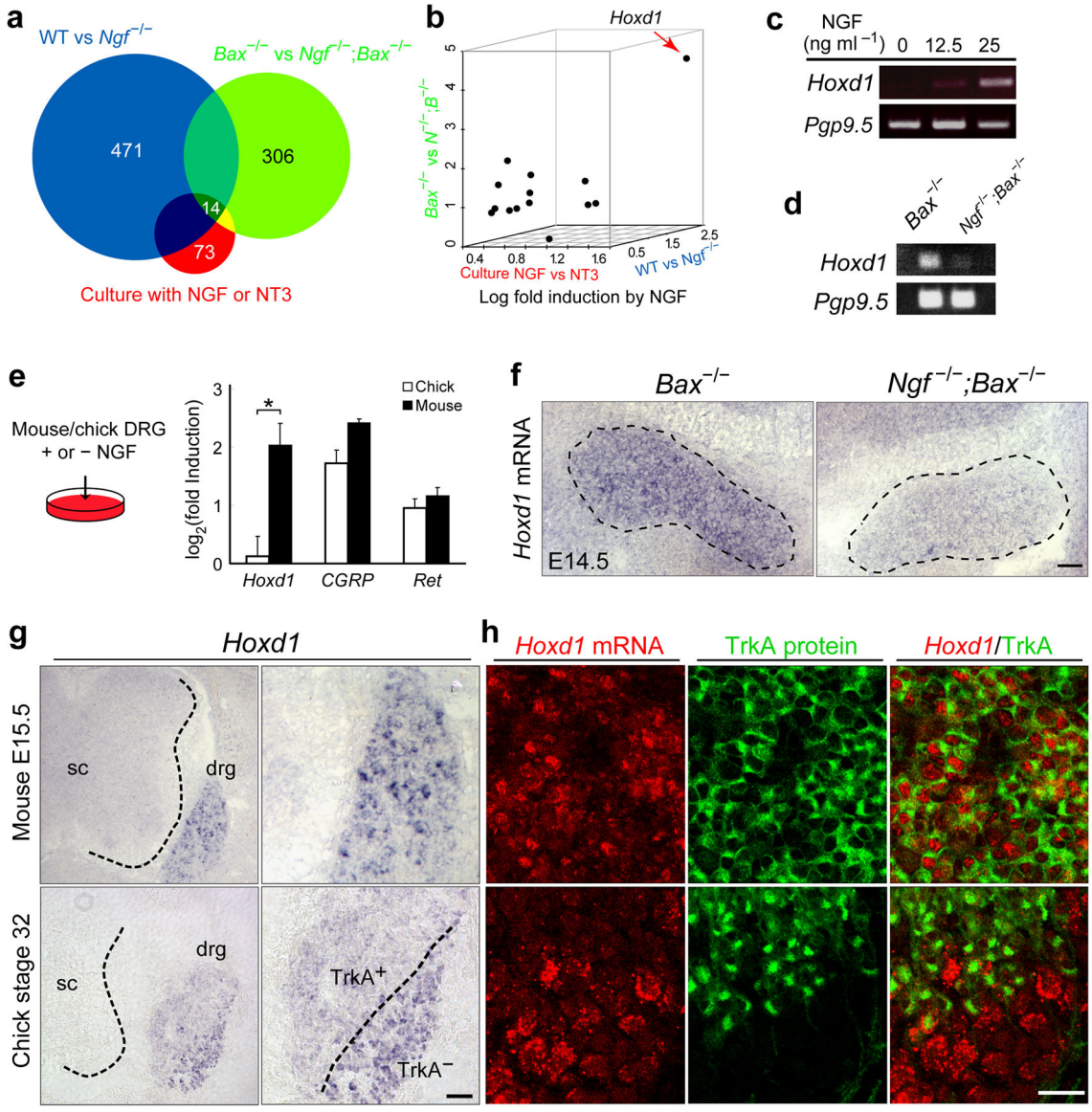


**Figure 1. NGF signaling induces *Hoxd1* expression in mammalian, but not avian, embryonic nociceptors**

**(a)** Diagram of the numbers of unique genes identified by the three microarray screens (at a loose cutoff of probability > 0.5 and fold change > 1.5). **(b)** The degree of mRNA level changes of the 14 genes identified by all three independent microarray screens, in log scale. **(c)** Application of NGF to cultured mouse DRG explants robustly induces transcription of *Hoxd1* within 24 hrs. **(d)** RT-PCR reactions comparing levels of *Hoxd1* mRNA in DRGs dissected from e14.5 $Bax^{-/-}$ and $Ngf^{-/-}$; $Bax^{-/-}$ embryos. **(e)** In parallel cultures of mouse and chick DRG explants, NGF induces robust transcription of canonical NGF-dependent genes (*CGRP* and *Ret*) in both species, but induces *Hoxd1* in mouse but not in chick DRGs as assessed by quantitative PCR. * $p < 0.05$ by Student's *t*-test (n = 3 independent batches of cultures for each condition). **(f)** *In situ* hybridization for *Hoxd1* mRNA in sections of developing DRGs of e14.5 $Bax^{-/-}$ and $Ngf^{-/-}$; $Bax^{-/-}$ embryos. Scale bar = 50 μm. **(g)**

Comparison of *Hoxd1* expression in DRGs and spinal cord of e15.5 mouse and stage 32 (e7.5) chick embryos. TrkA is a general marker for embryonic nociceptors. In chick DRGs, $TrkA^+$ nociceptors and TrkA non-nociceptors segregate into distinct topographic domains. sc, spinal cord. drg, dorsal root ganglion. Scale bar = 50 μm and 100 μm in low- and high-magnification panels, respectively. **(h)** Double fluorescent labeling of *Hoxd1* mRNA and TrkA protein in e15.5 mouse and stage 32 chick DRGs. Scale bar = 20 μm.

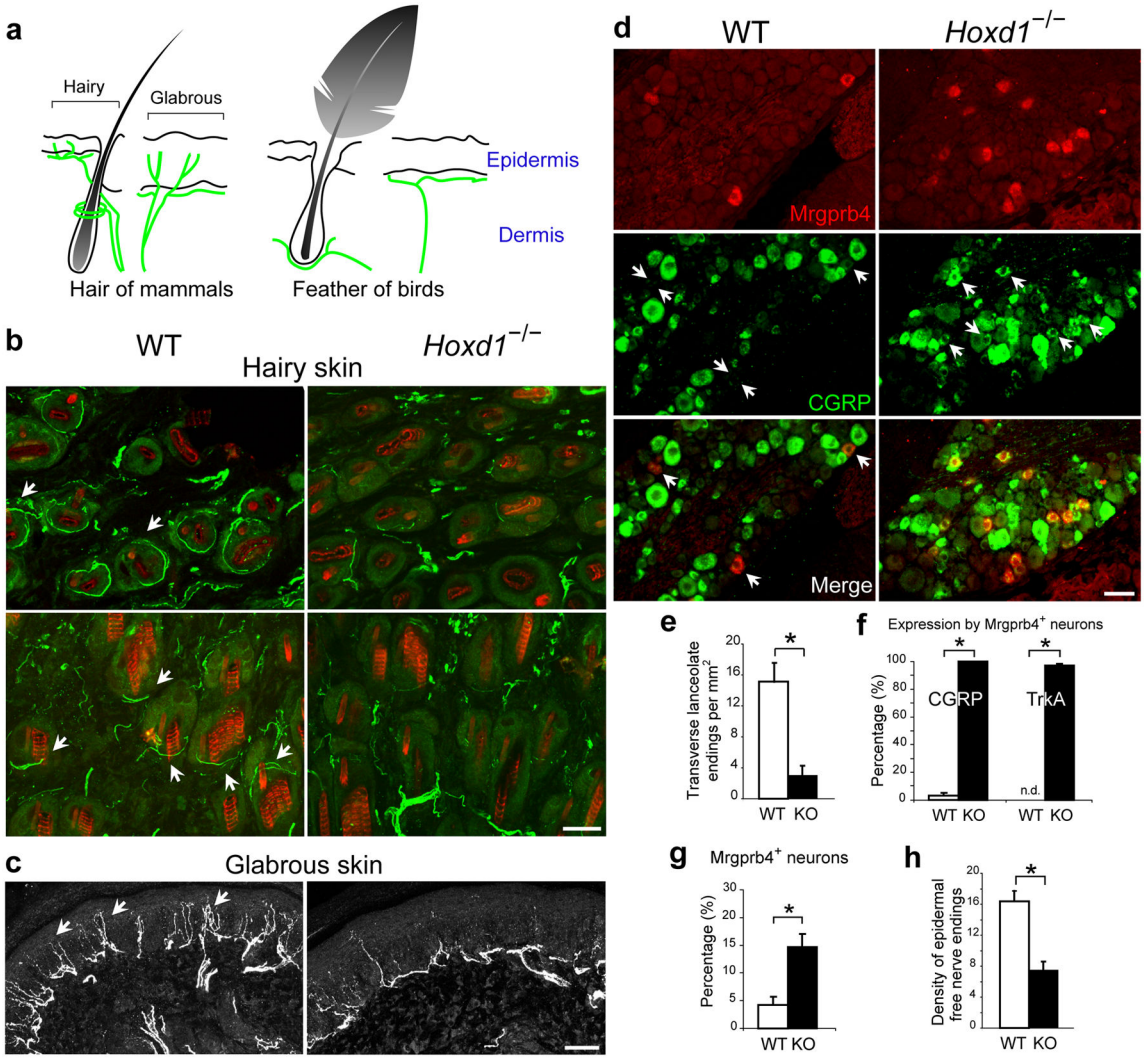


**Figure 2. *Hoxd1* instructs development of mammal-specific features of nociceptor axonal connections in the skin**

**(a)** Diagram showing the distinct patterns of nociceptor endings in the skin of mammals and birds. **(b)** Anti-peripherin staining of mouse hairy skin from proximal limb. Upper panels: transverse sections; lower panels: cross sections. (Hair is autofluorescent.) Scale bar = 40 μm and 50 μm in upper and lower panels, respectively. **(c)** A dramatic reduction in the number of nociceptor free nerve endings that penetrate the epidermis of hindlimb footpad glabrous skin of *Hoxd1*$^{-/-}$ mice was detected by anti-CGRP staining, which labels peptidergic nociceptors. Arrows indicate epidermal nociceptor endings. Scale bar = 40 μm. **(d)** Double fluorescent labeling of *Mrgprb4* mRNA and CGRP protein in L3 DRGs of WT and *Hoxd1*$^{-/-}$ mice. **(e)** Quantification of the number (±SEM) of transverse lanceolate endings per mm$^2$ skin area in serial sections of hindlimb back thigh hairy skin. * $p < 0.001$ by Student's *t*-test. **(f)** Percentage (±SEM) of Mrgprb4$^+$ neurons in WT and *Hoxd1*$^{-/-}$ mice that co-express *CGRP* or *TrkA*. * $p < 0.001$ by Student's *t*-test. **(g)** Quantification of the percentage (±SEM) of lumbar DRG neurons that express *Mrgprb4*. * $p < 0.001$ by Student's *t*-test. **(h)** Quantification of the average (±SEM) number of CGRP$^+$ free nerve endings

crossing the dermal-epidermal boundary per unit length (300 μm) of hindlimb footpad glabrous skin. * $p < 0.005$ by Student's *t*-test.

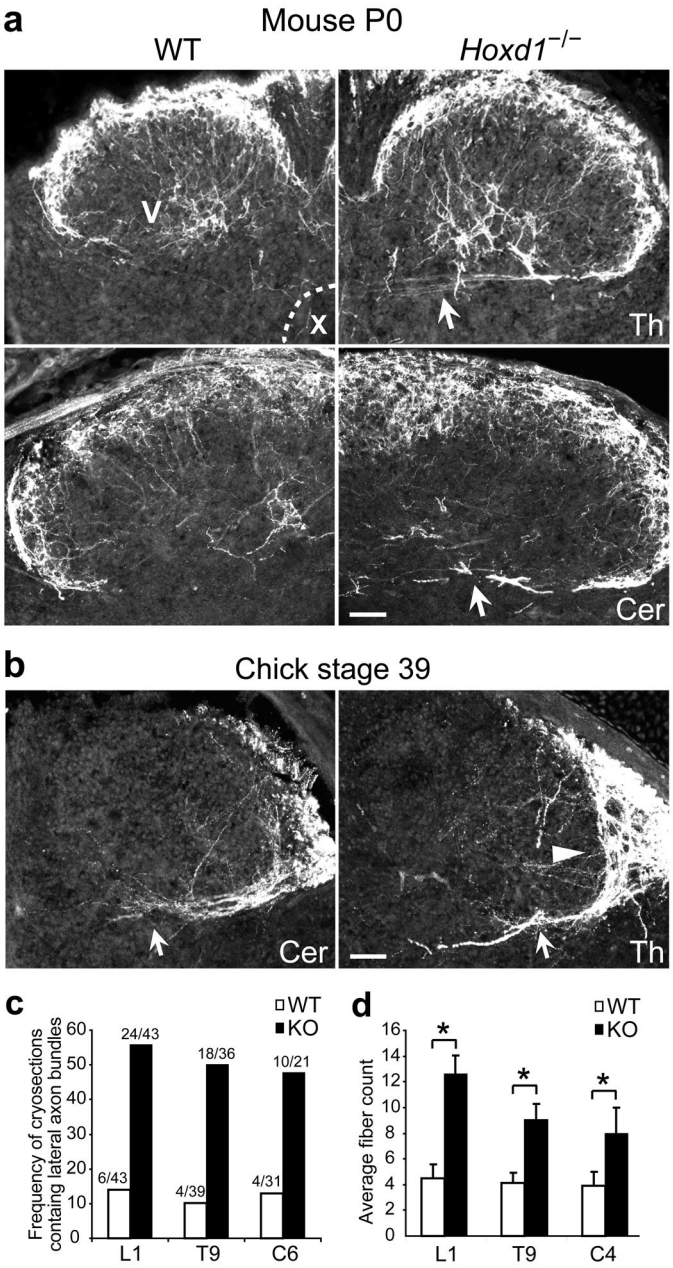


**Figure 3. *Hoxd1* controls a species-specific pattern of nociceptor axonal connectivity within the spinal cord**

**(a, b)** Anti-CGRP staining of the dorsal spinal cord of P0 mice and stage 39 (e13) chick. **(a)** Deep nociceptor central projections are abnormally increased in the spinal cord of *Hoxd1*$^{-/-}$ compared to WT mice revealed by anti-CGRP, a peptidergic nociceptor marker. More numerous deep projections were found at all axial levels, including cervical (Cer) and thoracic (Th) segments. V, lamina V; X, lamina X. Arrows point to aberrant deep projections extending into a region near the central canal (lamina X). Some CGRP$^{+}$ axons normally reach lamina V similarly in WT and *Hoxd1*$^{-/-}$ mice mostly from ventral projections emanating from the dorsal funiculus. **(b)** Anti-CGRP staining of nociceptor

central projections in stage 39 (e13) chick spinal cord at lower cervical and thoracic levels. Arrows indicate prominent horizontally-projecting deep nociceptor axon bundles in the spinal cord of the chick that resemble the abnormally increased fibers in *Hoxd1*$^{-/-}$ mice. Arrowhead indicates axon bundles that first project ventrally and then turn medially. Scale bar = 50 μm in **(a)** and **(b). (c)** Quantification of **(a)** comparing the fraction of 20μm sections of the spinal cord at different axial levels that contains bundles of deep nociceptor axons in WT (n = 5 animals) and *Hoxd1*$^{-/-}$ (n = 5 animals) mice. Numbers denote the numbers of sections examined. **(d)** Quantification of **(a)** comparing the average (±SEM) numbers of individual deep CGRP$^{+}$ fibers detected per section at different axial levels * $p < 0.05$ by Student's *t*-test. (n = 5 animals in each group.)

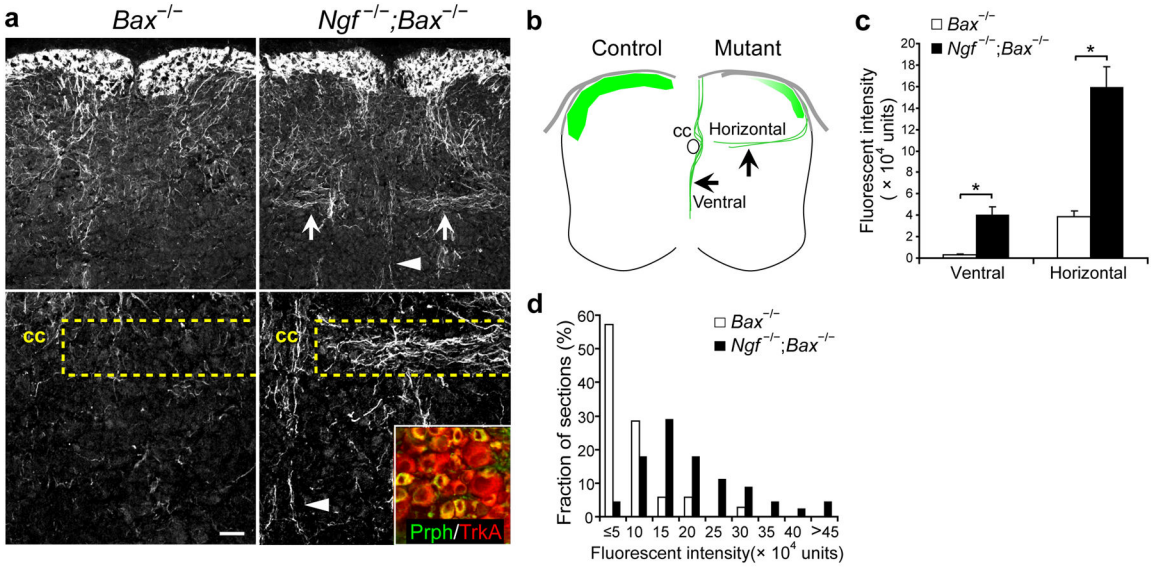


**Figure 4. NGF signaling controls a subset of central axonal projections of mammalian nociceptors in the spinal cord**

**(a)** Aberrant nociceptor axons, labeled with anti-Peripherin, project horizontally into deep regions of the spinal cord in *Ngf*$^{-/-}$; *Bax*$^{-/-}$ mice. Lower panels represent high-magnification of the images shown in upper panels. Dashed boxes indicate excessive deep nociceptor axons. cc, the central canal. **(Inset)** Peripherin is expressed at high levels in nociceptors[19,38]. Note that in *Ngf*$^{-/-}$; *Bax*$^{-/-}$mice, in addition to excessive horizontal projections, there is also an abnormally large number of aberrant deep nociceptor axons that project ventrally from the medial edge of the dorsal horn (arrowhead), some of which extend beyond the central canal. Scale bar = 60 μm and 30 μm in low- and high-magnification panels, respectively. **(b)** Diagram representing nociceptor central projection defects of *Ngf*$^{-/-}$; *Bax*$^{-/-}$ mice in comparison to *Bax*$^{-/-}$ controls. **(c, d)** Quantification of **(a). (c)** Fluorescent intensities are measured from areas represented by dashed rectangular boxes in **(a)**. Average (±SEM) fluorescent intensities of Peripherin$^{+}$ axons in deep ventral and horizontal projections are shown. * $p \leq 0.001$ by Student's *t*-test (n ≥ 5 animals in each group). **(d)** Fraction (%) of level-matched lumbar spinal cord sections that show anti-Peripherin fluorescent intensity in horizontal projections.

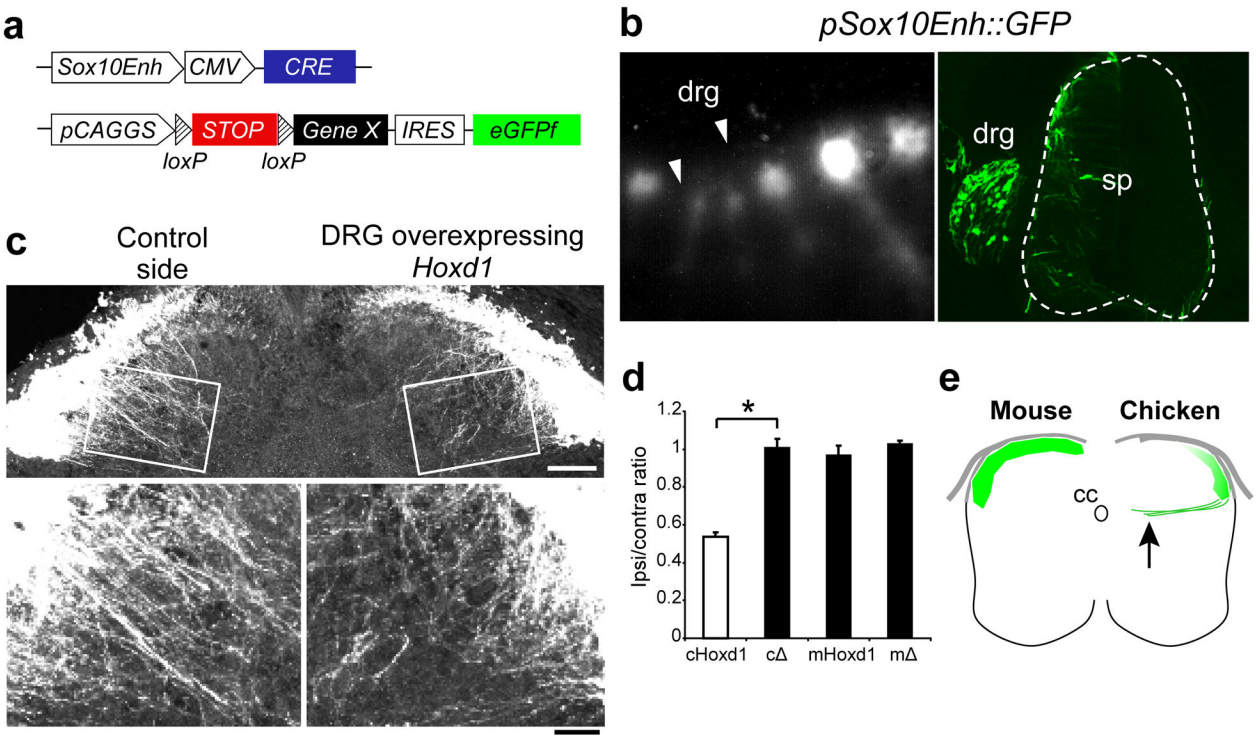


**Figure 5. Ectopic expression of *Hoxd1* in chick nociceptors impairs their axonal ingrowth into the lateral spinal cord**

**(a)** DNA constructs used for *in ovo* electroporation. **(b)** *Sox10* enhancer-driven *in ovo* electroporation directs ectopic gene expression in developing chicken DRGs but not in the spinal cord. Left panel: A whole-mount lateral view of GFP fluorescence in stage 26 chick embryos 3 days after electroporation. Right panel: Transverse sections of embryos processed as in the left panel, stained with anti-GFP. sp, spinal cord. drg, dorsal root ganglion. **(c)** The pattern of central projections of chick nociceptors is altered when *Hoxd1* is expressed in the chick DRG. Upper panel: A spinal cord section labeled with anti-TrkA at stage 35 (e9); Lower panels: high-magnification views of the boxed areas of the same spinal cord section. The left side is control, and DRGs of the right side of the embryo are electroporated with *Hoxd1*. Scale bar = 50 μm and 25 μm in low- and high-magnification panels, respectively. **(d)** Quantification of **(c)** shows the ratio between spinal cord areas occupied by $TrkA^+$ fibers in the electroporated side versus the control side. * $p = 0.0001$ by Student's *t*-test (n > 4 embryos for each group; sections are 25 μm thick and are sampled at least 200 μm apart). *cHoxd1*, chicken *Hoxd1* gene. *c*Δ, a chicken *Hoxd1* gene construct lacking the homeobox motif. *mHoxd1*, mouse *Hoxd1* gene. *m*Δ, a mouse *Hoxd1* construct lacking homeobox. **(e)** Diagram of the different patterns of spinal cord innervation by mammalian and avian nociceptors.

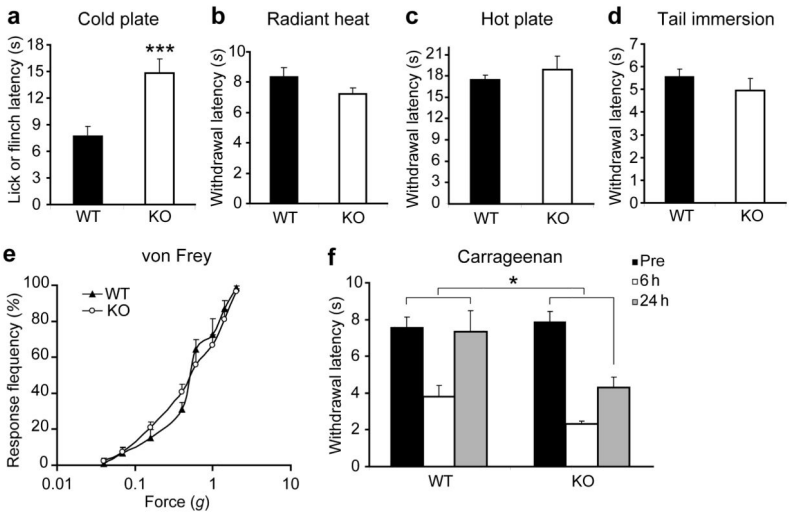


**Figure 6. Behavioral responses of *Hoxd1*$^{-/-}$ mice to somatosensory stimuli**

**(a)** *Hoxd1*$^{-/-}$ mice show a defect in their avoidance response to extreme cold. The paw licking or flinching response latency following exposure of mice to a 0°C cold plate is significantly increased in *Hoxd1*$^{-/-}$ mice compared to their WT littermate controls (n = 14 for WT, 13 for KO). *** $p < 0.001$ by Student's *t*-test. **(b–d)** *Hoxd1*$^{-/-}$ mice respond normally to acute noxious thermal stimuli. Response latencies in **(b)** the Hargreaves (n = 12 for WT, 11 for KO), **(c)** hot-plate (50°C; n = 9 per genotype) and **(d)** tail-immersion (50°C; n = 9 per genotype) tests do not differ between WT and *Hoxd1*$^{-/-}$ mice. **(e)** The paw withdrawal threshold of *Hoxd1*$^{-/-}$ mice to punctate mechanical stimuli (von Frey test) is comparable to that of WT mice (n = 12 per genotype). **(f)** *Hoxd1*$^{-/-}$ mice show prolonged thermal hyperalgesia 24 hours after intraplantar injection of 1% carrageenan as compared with WT mice (10 μl; n = 9 per genotype). Pre, preinjection. Data are presented as Mean (±SEM). * $p < 0.01$ Two-way ANOVA.